Journal of Physics: Conference Series

Synthesis of Ni_2B nanoparticles by RF thermal plasma for fuel cell catalyst

To cite this article: Y Cheng *et al* 2014 *J. Phys.: Conf. Ser.* **518** 012026

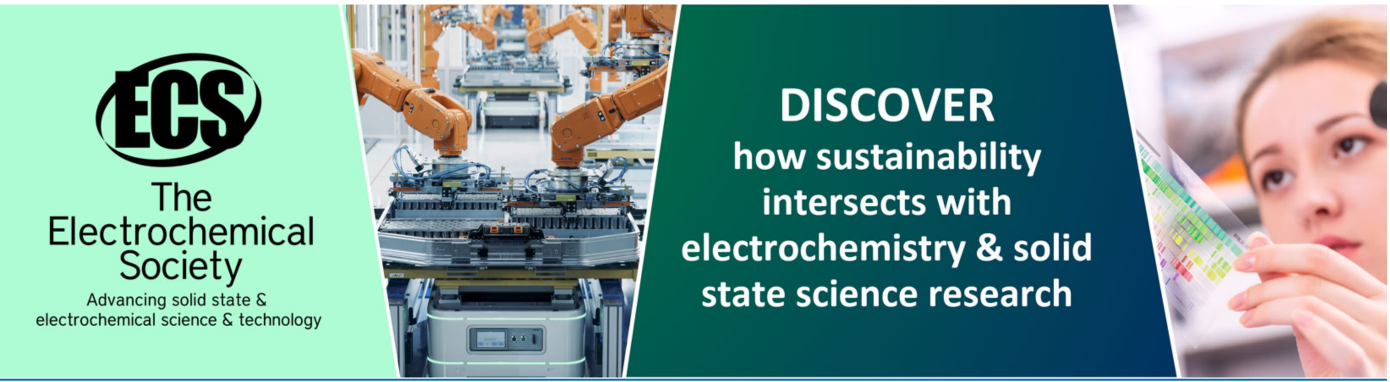

Journal of Physics: Conference Series **518** (2014) 012026 doi:10.1088/1742-6596/518/1/012026

Synthesis of Ni_2B nanoparticles by RF thermal plasma for fuel cell catalyst

Y Cheng[1], M Tanaka[1], T Watanabe[1,2], S Y Choi[3], M S Shin[3] and K H Lee[3]

[1] Dept. Environmental Chemistry and Engineering, Tokyo Institute of Technology, 4259 Nagatsuta-cho, Midori-ku, Yokohama 226-8502, Japan
[2] Dept. Chemical Engineering, Kyushu Univ., 744 Motooka, Nishi-ku, Fukuoka 819-0395, Japan
[3] Plasma Nano Division, Cheorwon Plasma Research Institute, 4620 Hoguk-ro, Galmal-eup, Cheorwon-gun, Gangwon-do, 269-802, Korea

E-mail: watanabe@chemenv.titech.ac.jp

Abstract. The catalyst of Ni_2B nanoparticles was successfully prepared using nickel and boron as precursors with the quenching gas in radio frequency thermal plasmas. The generating of Ni_2B needs adequate reaction temperature and boron content in precursors. The quenching gas is beneficial for the synthesis of Ni_2B in RF thermal plasma. The effect of quenching rate, powder feed rate and boron content in feeding powders on the synthesis of nickel boride nanoparticles was studied in this research. The high mass fraction of 28 % of Ni_2B nanoparticles can be generated at the fixed initial composition of Ni:B = 2:3. Quenching gas is necessary in the synthesis of Ni_2B nanoaprticles. In addition, the mass fraction of Ni_2B increases with the increase of quenching gas flow rate and powder feed rate.

1. Introduction

The development of novel materials is a fundamental point of chemical research, which has been promoted by progress in nanotechnology. Because of their refractory nature, resistances to sulfur poisoning, and desulphurization ability in organic synthesis and catalytic properties [1], metal borides have been considered as potentially desirable catalysts. Among various metal borides, nickel boride, Ni_2B, is regarded as a potential industrial catalyst for hydrogenation reactions [2]. Previous investigations indicated that nickel boride nanoparticle is useful in catalysts for electrodes of fuel cell [2, 3]. The remarkable catalytic activity of nickel boride has been attributed to the ability of boron to donate an electron to nickel [4]. Several routes have been proposed to synthesize Ni_2B, i.e., sodium borohydride, boronizng of pure nickel by the powder-pack method [5] and ball milling of element components [6]. To the best of our knowledge, there are hardly any reports on Ni_2B nanoparticles prepared by Radio frequency (RF) thermal plasma route, which is a great challenge.

RF thermal plasmas has many unique merits including high enthalpy, high chemical reactivity, large plasma volume, long residence time, and selective oxidation or reduction atmosphere according to the required chemical reactions. The high temperature of thermal plasma enables the evaporation of a large amount of raw materials even with high melting and boiling temperatures [7,8]. The formation of nanoparticles in supersaturated state by homogeneous nucleation and heterogeneous condensation can be accomplished due to the rapid quenching rate in the tail flame [9-11]. Furthermore, it is available to synthesize nanoparticles with high purity by RF thermal plasma, because the thermal plasma is generated in the torch without an internal electrode.

Few investigations for the synthesis nickel boride Ni_2B by RF thermal plasma have been reported so far. The purpose of this study is to examine the effect of experimental parameters on the synthesis of nickel boride nanoparticles in RF thermal plasma. The experiments were carried out with controlling the powder feed rate, boron content in feeding powders and quenching gas flow rate to produce expected Ni_2B nanoparticles. Adequate phase composition and temperature play the important role in the synthesis of Ni_2B nanoparticles. The phase composition of product and mass fraction of nickel boride were measured by X-ray diffractometry (XRD).

2. Experimental procedure

The schematic apparatus of RF thermal plasma system for the production of boride nanoparticles is shown in figure 1. The system consists of a plasma torch, a reaction chamber, a particle collection filter, and a power supply. The plasma torch is composed of a water-cooled quartz tube and a water-cooled induction coil (3 turns), coupling its electromagnetic energy to the plasma at a frequency of 4 MHz. The feeding powders were nickel (particle size: 45 μm, purity: 99.9%, Kojundo Chemical Laboratory Co. Ltd., Japan) and crystalline boron (particle size: 45 μm, purity: 99%, Kojundo Chemical Laboratory Co. Ltd., Japan). Nickel and boron particles were mixed at the fixed initial molar composition before they were injected into the RF thermal plasma through the powder feeder.

After the precursors were introduced into the plasma region with argon carrier gas, they were instantaneously evaporated due to the very high enthalpy of the RF thermal plasma. Therefore, the nickel boride nanoparticles are synthesized from the gas phase.

The operating conditions are summarized in Table 1. Argon was introduced as the carrier gas of 3 L/min, the inner gas of 5 L/min, the sheath gas of 60 L/min and the quenching gas. Helium of 5 L/min was also used as the sheath gas. The sheath gases were injected from the outer slots of the plasma torch located between the injection tube and the quartz tube to protect the inner surface of the quartz tube and to stabilize the plasma. The powder feed rate was 0.1, 0.2 and 0.5 g/min and the molar content of boron in the feeding powder was controlled from 33.3 to 75.0 at. %. The quenching gas flow rate was from 5 to 20 L/min. The RF plasma was operated at the fixed input power of 30.0 kW under atmospheric pressure.

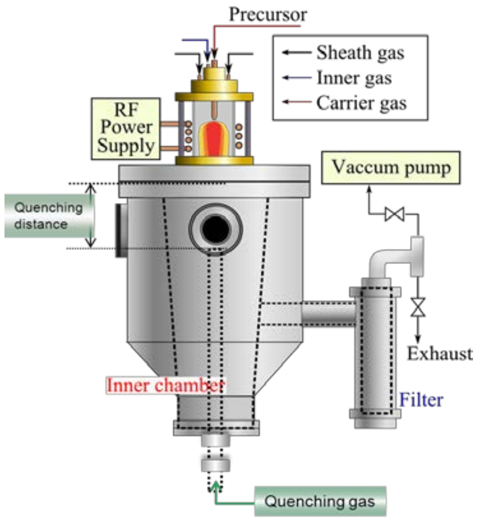

Figure 1. Experimental set-up of RF thermal plasma for the synthesis of metal boride nanoparticles.

The synthesized nanoparticles were characterized for phase identification by XRD (MXP3TA, Mac Science). The crystalline size was calculated from the full widths at the half maximum (FWHM) of the most intensive diffractions according to the Scherrer's equation. Quantitative phase analysis by using XRD data was carried out based on the adiabatic method [12]. This method evaluates the mass fraction of each phase from the relative intensity of the diffraction peak of product. The mass fraction of *X* phase can be calculated by following equation (1)

$$W_X = \frac{I_X}{K_A^X \sum_{X=A}^{N} \frac{I_X}{K_A^X}} = \frac{I_X}{K_{Ni}^X \cdot \left(\frac{I_{Ni}}{Ki} + \frac{I_{NiB}}{K_{Ni}^{NiB}} + \frac{I_{Ni_4B_3}}{K_{Ni}^{Ni_4B_3}} + \frac{I_{Ni_2B}}{K_{Ni}^{Ni_2B}} + \frac{I_{Ni_3B}}{K_{Ni}^{Ni_3B}} \right)} \tag{1}$$

where, *X* (= Ni, NiB, Ni_4B_3, Ni_2B, Ni_3B) denotes each phase in the product. I_X presents the intensity of *X* phase in the product from the XRD spectrum. K_A^X is the ratio of the reference intensity ratio (*RIR*) values of *X* phase to that of the reference phase *A*, *i.e.*, $K_A^X = RIR_X/RIR_A$. In the experimental measurement of Ni-B system, peaks for Ni, NiB, Ni_4B_3, Ni_2B and Ni_3B were identified in XRD spectrum, and Ni was selected as the reference materials. Based on the powder diffraction file cards, *RIR* values for Nb, NiB, Ni_4B_3, Ni_2B and Ni_3B are determined to be 7.41, 2.88, 1.43, 5.68 and 1.45, respectively.

Table 1. Operating condition for the synthesis of niobium boride nanoparticles.

Process parameters	Value
Sheath gas and flow rate	Ar-He (60:5) 65 L/min
Inner gas and flow rate	Ar 5 L/min
Carrier gas and flow rate	Ar 3 L/min
Quenching gas flow rate	Ar 5, 10 and 20 L/min
Plasma power	30.0 kW
Reactor pressure	101.3 kPa
Frequency	4 MHz
Powder Feed rate	0.1-0.5 g/min
Boron molar content in feeding powder	33.3-75.0 at.%

3. Results and discussion

XRD spectra of as-prepared product with or without quenching gas at powder feed rate of 0.2 g/min are displayed in figure 2. Figure 3 displays the magnification of figure 2 from 40º to 50º. The peaks of Ni_2B and Ni_4B_3 can be identified with quenching gas. The peaks of Ni_3B are observed without quenching gas. Generating Ni_2B needs some special temperature and phase composition according to the phase diagram [13]. Quenching gas can stop the reaction at certain temperature. Therefore, Ni_2B was prepared with adequate quenching gas and phase composition.

Figure 4 shows the XRD spectra of product at the fixed initial composition with different quenching gas flow rates. From the XRD measurement, Ni, Ni_4B_3 and Ni_2B were identified. Gibbs free energy of Ni_2B is negative, indicating Ni_2B can be generated spontaneously and easily. The highest intensity of the peak was unreacted Ni, while the dominant product is Ni_4B_3. This XRD result indicates that the synthesis of Ni_2B nanoparticle is difficult.

Figure 5 indicates the relationship between the mass fraction of each phase in the products and quenching gas flow rate. The mass fraction of Ni_2B in product increases with increasing quenching gas flow rate. Adequate quenching gas can stop the reaction at certain temperature, which can improve the

Journal of Physics: Conference Series **518** (2014) 012026 doi:10.1088/1742-6596/518/1/012026

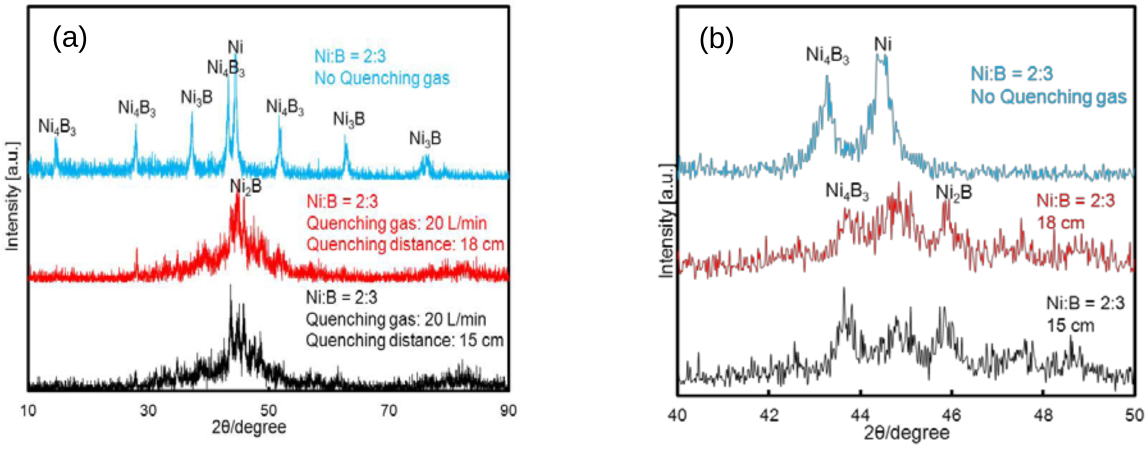

Figure 3. XRD patterns of product with different quenching distance at Ni:B = 2:3 (a) and magnified patterns (b).

generating of Ni_2B nanoparticles. The unreacted boron, which was not reacted with nickel but evaporated, increases with increasing the quenching gas flow due to shorter residence time, resulting from the higher temperature gradient. The enthalpy of the complete evaporation was about several hundred J/s when the input power was adjusted at 30 kW. The energy efficiency for the evaporation was around 2%. Complete evaporation of the raw materials was confirmed by SEM observation of the collected powders.

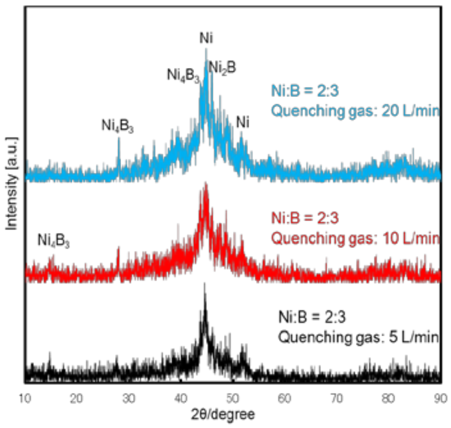

Figure 4. XRD patterns of product with different quenching gas flow rate at Ni:B = 2:3

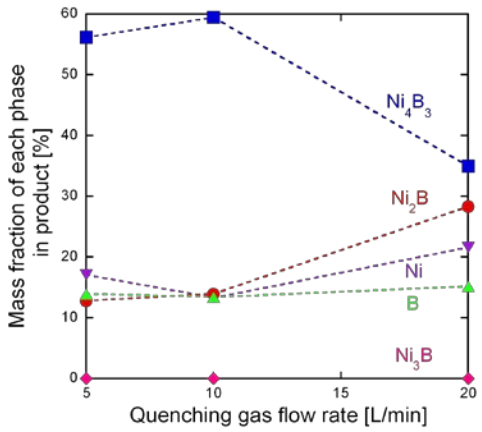

Figure 5. Mass fraction of each phase in product with different quenching gas flow rate at Ni:B = 2:3

Figure 6 displays the XRD patterns of product with different boron molar content in feeding powders at fixed quenching gas flow rate. In boron poor condition, the dominant product is Ni_3B. The peak of unreacted Ni has the highest intensity in boron rich condition, while Ni_3B are not observed. The highest intensity of Ni_2B in product is generated with the phase composition of Ni:B = 2:3.

The effect of boron molar content in feeding powders on the mass fraction of each phase in product is shown in figure 7. The highest mass fraction Ni_2B in product is observed with the initial composition of Ni:B = 2:3. In the boron poor condition, Ni_2B cannot be generated, while the mass fraction of Ni_2B decreases with increasing boron content in feeding powders in boron rich condition. We can get the high mass fraction of Ni_4B_3 with the initial composition of Ni:B = 1:2. Adequate temperature and boron content improve the synthesis of Ni_2B and Ni_4B_3. The synthesis of Ni_2B is the most difficult compared with that of Ni_4B_3 and Ni_3B due to the narrow composition region in phase diagram. The Ni_3B were generated in the boron poor condition. In addition, the mass fraction of unreacted boron increases with the increase of boron content in feeding powders because of larger amount boron in feeding powders.

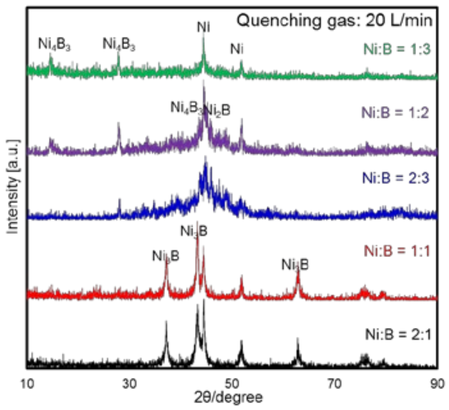

Figure 6. XRD patterns of product with different boron molar content in feeding powders.

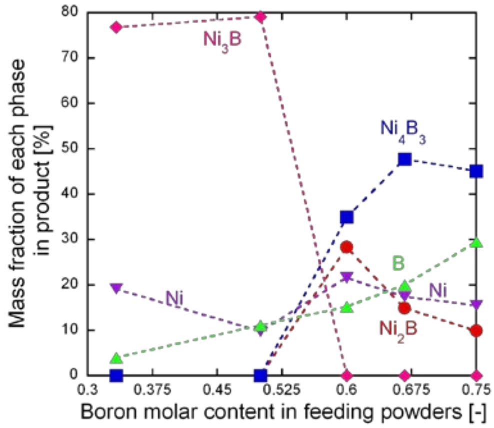

Figure 7. Mass fraction of each phase in product with different boron molar content in feeding powders.

Figure 8 displays the XRD spectra of product with different powder feed rate at the fixed initial composition of Ni:B = 2:3. With the low powder feed rate, Ni_3B can be identified. With the high powder feed rate, only the peaks of Ni and Ni_2B are observed.

The relationship between the powder feed rate and the mass fraction of each phase in product is observed in figure 9. The high mass fraction of Ni_2B and Ni_4B_3 in product is prepared at the powder feed rate of 0.2 g/min.

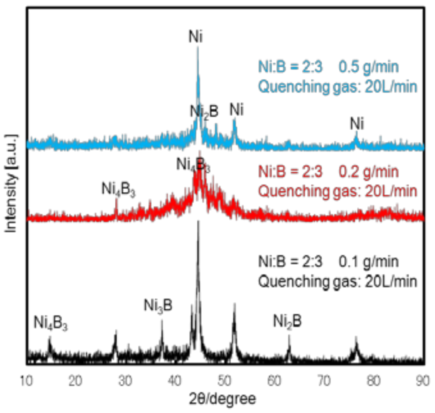

Figure 8. XRD patterns of product with different powder feed rate at Ni:B = 2:3

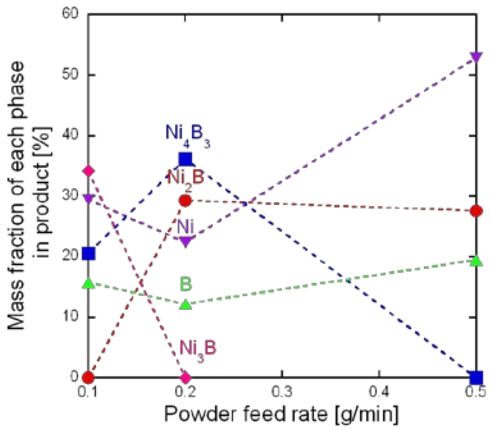

Figure 9. Mass fraction of each phase in product with different powder feed rate at Ni:B = 2:3

5. Conclusions

Experimental study were carried out to prepare nickel boride nanoparticles and to investigate the effect of powder feed rate, quenching gas flow rate and the boron molar content in feeding powders on the phase composition of product in RF thermal plasma. In this work, nickel boride Ni_2B nanoparticles were successfully synthesized in RF thermal plasma. The quenching gas and boron content in feeding powders play an important role in the controlled synthesis of nickel boride nanoparticles in RF thermal plasma. The highest mass fraction Ni_2B in product is observed in the initial composition of Ni:B = 2:3 with quenching gas flow rate of 20 L/min. The high mass fraction of Ni_4B_3 in the initial composition of Ni:B = 2:3 with quenching gas flow rate of 10 L/min. The Ni_3B were generated only in the boron poor condition.

References

[1] Ganem B, et al. 1986 *Chem. Rev.* **86** 763
[2] Brown HC, et al. 1963 *J. Amer. Chem. Soc.* **85** 1005
[3] Jasinski R 1963 Symposium on Fuel Cells, Division of Fuel Chemistry, 145th National Meeting of the American Chemical Society, N.Y., Sept. 8-13,
[4] Okamoto Y, et al. 1979 *J. Chem. Soc.* **75** 2027
[5] Ueda N, Mizukoshi T, Demizu K, Sone T, Ikenaga A and Kawamoto M 2000 *Surf. Coat. Tech*. **126** 25
[6] Corrias A, Ennas G, Marongiu G, Musinu A, Paschina G and Zedda D 1995 *Mat. Sci. Eng. A.* **204** 211
[7] Watanabe T, Nezu A, Abe Y, Ishii Y and Adachi K 2003 *Thin Solid Films* **435** 27
[8] Szepvolgyi J, Markovic Z, Scheier P and Feil S 2006 *Plasma Chem. Plasma Process.***26** 597
[9] Shigeta M and Watanabe T 2005 *J. Mater. Res.***20** 2801
[10] Desilets M, Bilodeau. JF and Proulx P 1997 *J. Phys. D: Appl. Phys*.**30** 1951
[11] Gonzalez NYM, Morsli ME and Proulx P 2008 *J. Therm. Spray Technol.***17** 533
[12] Cheng YY and Watanabe T 2011 *J. Chem. Eng.Jpn.***44** 583
[13] Passerone A, Muoloa ML, Valenza F and Kaufman L 2010 *Comput. Coupl. Phase Diag. Thermochem.* **34** 6